Applied Thermal Engineering 62 (2014) 69–79

Contents lists available at ScienceDirect

Applied Thermal Engineering

journal homepage: www.elsevier.com/locate/apthermeng

Experimental study of a domestic thermoelectric cogeneration system

X.F. Zheng [a], C.X. Liu [a, b], R. Boukhanouf [a], Y.Y. Yan [a, *], W.Z. Li [b]

[a] Energy and Sustainability Research Division, Faculty of Engineering, University of Nottingham, University Park, Nottingham NG7 2RD, UK
[b] School of Power and Energy, Dalian University of Technology, Dalian 116024, China

HIGHLIGHTS

- A thermoelectric cogeneration system uses both converted heat and unconverted heat.
- This system can deliver energy utilisation efficiency up to 80%.
- Thermal efficiency varies with operating temperature due to unstable matching load.
- The fluid-filled heat exchanger enables the system to store and spread heat.

ARTICLE INFO

Article history:
Received 14 March 2013
Accepted 4 September 2013
Available online 25 September 2013

Keywords:
Thermoelectric cogeneration
Thermal efficiency
Domestic

ABSTRACT

Thermoelectric application for power generation does not appear to be appealing due to the low conversion efficiency given by the current commercially available thermoelectric module. This drawback inhibits its wide application because of the overall low thermal efficiency delivered by typical thermoelectric applications. This paper presents an innovative domestic thermoelectric cogeneration system (TCS) which overcomes this barrier by using available heat sources in domestic environment to generate electricity and produce preheated water for home use. This system design integrates the thermoelectric cogeneration to the existing domestic boiler using a thermal cycle and enables the system to utilise the unconverted heat, which represents over 95% of the total absorbed heat, to preheat feed water for domestic boiler. The experimental study, based on a model scale prototype which consists of oriented designs of heat exchangers and system construction configurations. An introduction to the design and performance of heat exchangers has been given. A theoretical modelling for analysing the system performance has been established for a good understanding of the system performance at both the practical and theoretical level. Insight has also been shed onto the measurements of the parameters that characterise the system performance under steady heat input. Finally, the system performance including electric performance, thermal energy performance, hydraulic performance and dynamic thermal response are introduced.

1. Introduction

In most developed countries with temperate climate, heat for space heating and domestic hot water is often provided by burning gas or oil in a boiler or furnace. Current condensing boilers are highly efficient achieving thermal efficiencies in excess of 90% with combustion gases rejected at dew point temperature. Despite a growing market for condensing boilers, a large number of old boilers are still being used with thermal efficiency as low as 55%, resulting in large energy loss [1].

Thermoelectric modules, consisting of pairs of p-type and n-type semiconductor materials forming a pair of thermocouple, generate electricity when a temperature difference is established across the module. Thermoelectric devices have found a wide range of applications including power generation, heat recovery and thermal sensing. These applications span a wide range of industries such as transport [2,3], process industries [4–6], medical [7,8] and space [9]. Many efforts have been made in the development of advanced thermoelectric materials with high conversion efficiency to enhance the potential of a wider range of applications [10–13]. According to operating temperature, thermoelectric materials are classified into three categories: low temperature, intermediate temperature and high temperature thermoelectric. The low temperature type, which includes alloys based on bismuth in combinations with antimony, tellurium or selenium, utilises heat from

* Corresponding author. Tel.: +44(0)115 951 3168.
E-mail address: yuying.yan@nottingham.ac.uk (Y.Y. Yan).

1359-4311/$ – see front matter © 2013 Elsevier Ltd. All rights reserved.
http://dx.doi.org/10.1016/j.applthermaleng.2013.09.008

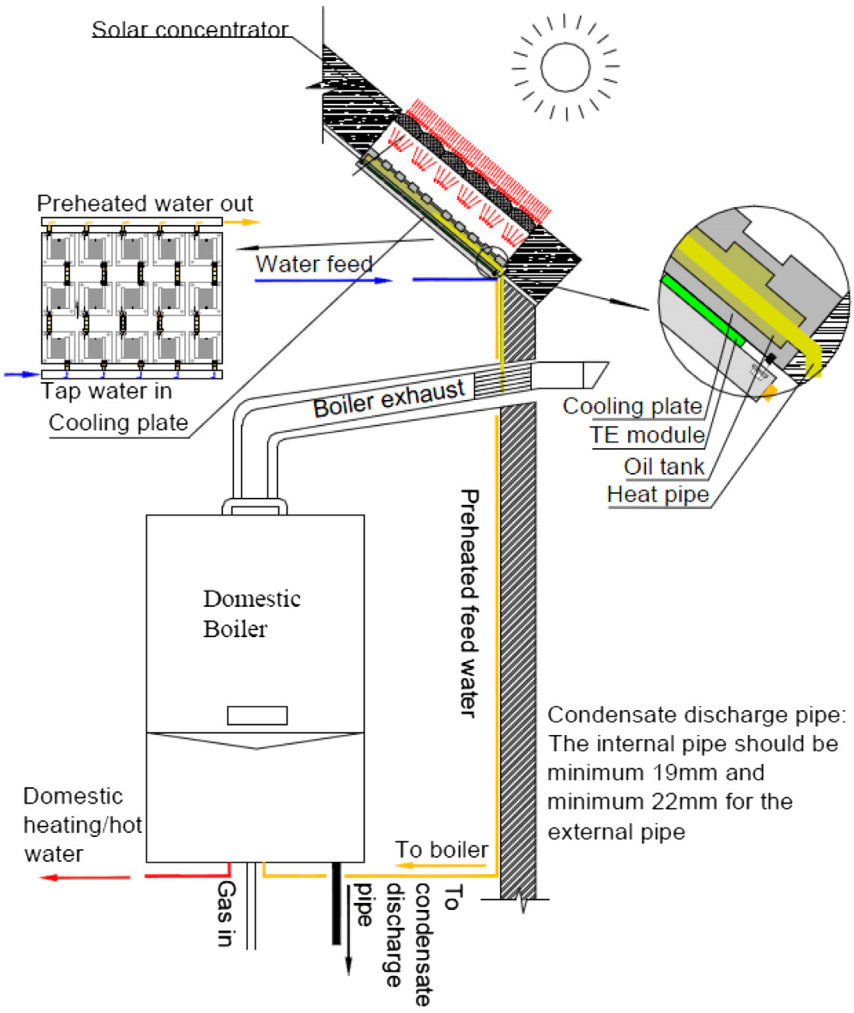

Fig. 1. Concept diagram of domestic thermoelectric cogeneration system.

warm/hot water or general waste heat by operating up to 523 K, while the latter two which include the alloys of lead telluride and silicon germanium are oriented for incineration/steel plants and automobile exhaust, respectively [14]. Their operating temperatures can reach up to 850 K and 1300 K. Suitable application of thermoelectric material is generally referred to large electrical power factor, good cost effectiveness and being environmentally friendly. For high operating temperature, modules with segmented thermoelectric elements have larger average figure-of-merit ZT over a large temperature drop compared to those using same alloy in the element [15]. The thermoelectric efficiency reached as high as 20% operating between 300 K and 975 K [16]. For applications in cogeneration for domestic buildings with heat source temperature about 473 K, Bi_2Te_3 has been selected for its high figure of merit, ZT.

The main advantages that boast thermoelectric devices are being static, compact, and low maintenance cost. However, low conversion efficiency has confined their application to specialised niche markets. One of these markets is generating electrical power in buildings located in inaccessible remote areas. For instance, back in 1996, the Swedish Royal Institute of Technology [17] developed a thermoelectric stove to provide small amounts of power to residential houses in the remote northern areas of the country where grid connection is prohibitively expensive. Recent works on thermoelectric stoves include those of Champier [18], Nuwayhid [19] and Mastbergen [20], which recover waste heat from cooking stove to generate electricity to power fan or lamp.

Because domestic boilers rely on grid connection for operation, Daniel [21,22] attempted to develop a self-powered domestic boiler using thermoelectric generators by integrating the thermoelectric modules between the combustion chamber and the water channel in the boiler enclosure. Thermoelectric generators were also thought of as direct contenders to replacing diesel gensets for power generation in off-grid buildings, eliminating noise, and high maintenance that characterise internal combustion engines. Commonly, the heat sink is an assembly of a finned heat exchanger and fan that removes heat via forced convection.

The thermal performance of the thermoelectric devices for power generation-only applications remains, however, poor with maximum efficiency below 5% [14]. This means 95% of the fuel energy content is rejected as low grade heat. Therefore, recovering rejected heat for useful utilisation for space heating and domestic hot water as part of a thermoelectric cogeneration system would make thermoelectric more attractive as overall thermal efficiency could be increased up to 100%, which was discussed by Gao in Ref. [23]. In a later time, this concept was initially proved in a different work by the author at an earlier time [24], which demonstrated a practical achievement of thermal efficiency at up to 80%. Qiu [25] developed a thermoelectric power generation system which generates electricity and hot water by burning natural gas in a furnace. Relying on the supply of natural gas, its operation is suitable for the applications which are purposefully designed for using the natural gas as the primary fuel. In the first stage study [24], the author

proposed the concept of cogeneration system which uses the heat from boiler exhaust and solar power in the UK residential houses. A potential benefit has been prospected for supplementing the domestic energy need and improving the energy efficiency in the UK residential house on the basis of the available heat from boiler waste and solar energy.

This paper presents the further investigation to this concept with great details in system performance and technical aspect in heat exchangers. It attempts to address problems of heat transfer at the interface of the thermoelectric module in micro-scale cogeneration systems. As previously reviewed, some studies have been conducted to the TE power generation in fire stoves and domestic heating jacket. But there is no similar experimental study that has been done to its application in the domestic boilers so far. This study, based on an innovative attempt in improving the domestic environment in the typical temperate regions where domestic boiler is widely used, will present the potential benefit of using this domestic TCS.

2. Description of the system

As shown in Fig. 1, the primary heat source of the thermoelectric cogeneration is the waste heat from boiler exhaust. A cooling fluid is circulated through a compact heat exchanger on the cold side of the TE module to convert the recovered heat to electricity and provide heat for the building. The system is also capable of using solar energy absorbed by a solar collector mounted on the roof of a building whereby solar energy is absorbed and supplied to the thermoelectric module hot side. This can be achieved by direct utilisation or indirect utilisation of solar energy, depending on the heat exchanger design. The heat absorbed from the two aforementioned heat sources can be used to generate “free” electricity and attendant heat is used for heating purposes, increasing the overall energy utilisation efficiency of the boiler. However one of the challenging designs is to overcome limitations of heat transfer to and from the thermoelectric module.

Fig. 1 shows the concept of domestic thermoelectric cogeneration system which absorbs heat from boiler waste and solar energy using a hot side heat exchanger. The heat rejected from the cold side of thermoelectric modules is taken away by the cooling plate which is connected to the boiler to provide preheated water. The hot side heat exchanger is specifically designed for absorbing the heat from boiler waste and solar energy. Two modules are studied as described in Fig. 2. Fig. 2A shows a concept of indirect use the heat in which heat transfer oil absorbs the heat from boiler waste and solar energy. The oil is heated up by the absorbed energy and flows through the TE module to proceed with the energy conversion and water preheating. Fig. 2B shows the direct use of heat in which the solar energy and boiler waste heat is used directly to heat the TE hot side. The selection can be made according to the availability of heat sources and requirements on the system response time. Solar concentration measures can also be taken to promote the temperature level at the heat source side.

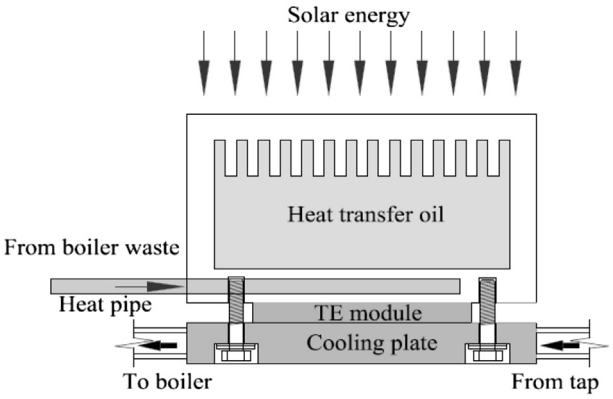

Fig. 3. Schematic diagram of the TE co-generator assembly.

3. Design of the TE co-generator

The factors that significantly influence the thermal efficiency of thermoelectric application include the boundary conditions of hot and cold sides, the usage of thermodynamic cycles and thermoelectric materials. Among which, the thermal boundary conditions of hot and cold side are involved with the available ways of extracting the heat from heat sources and dissipating the unconverted heat from the cold side which significantly influences the efficiency. This leads to the technical aspects of heat exchange design. The heat sourcing and heat dissipation determines the heat flux of the system, which takes us to the consideration in the design of thermodynamic cycles which can offer the promise of substantially higher efficiency.

The thermoelectric co-generator, consisting of a hot side heat exchanger, a cooling plate and a thermoelectric module, is intended to use heat from external solar radiation source and waste heat from a domestic combustion appliance. This is achieved by mounting the TE module between the external surface of the hot side heat exchanger and the cooling plate, as shown in Fig. 3.

Crinkle washer, flat metal washer and fibre washer are used to accommodate the thermal expansion and reduce thermal bypass

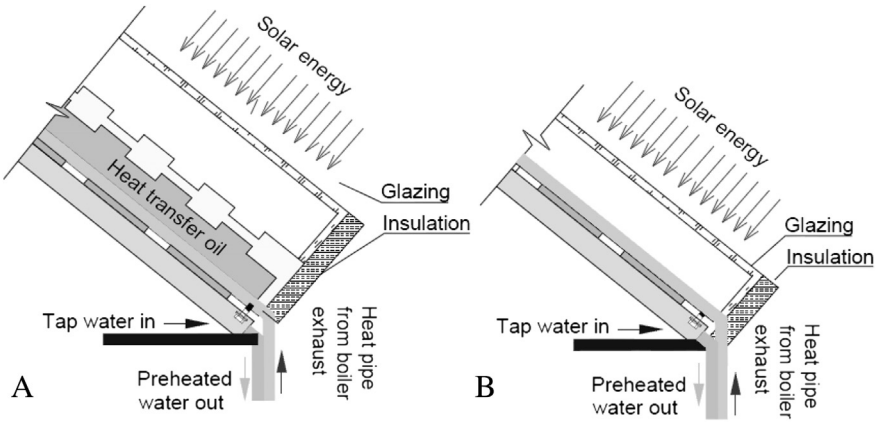

Fig. 2. Schematic diagram of hot side heat exchanger.

through the stainless steel screws. For a good thermal contact, the recommended compression of a thermoelectric assembly is 10–21 kg per square centimetre (150–300 PSI), corresponding to torque value in the range of 0.33 Nm–0.66 Nm. A series of tests have been carried out under the torque value of 0.30 NM, 0.35 NM, 0.40 NM, 0.45 NM and 0.50 NM to investigate the impact of pressure load to the system performance, the optimum pressure load has been identified at 0.40 NM, corresponding to the pressure load 180 PSI.

Fig. 4 compares the thermal cycle of conventional thermoelectric system (Fig. 4a) and the domestic TCS (Fig. 4b). The domestic TCS distinguishes itself from the conventional system, which wastes the unconverted heat to the ambient environment, by reusing the unconverted heat to preheat boiler feel water to reduce the fuel need for water heating. This is achieved by using the oriented cooling design as the cooling plate, which is further introduced in subsection 3.2. Meanwhile, the fluid-filled hot side heat exchanger enables the system to accommodate dual heat source (in this context, boiler waste heat and solar power) by bridging the two heat sources via the heat transfer oil.

3.1. Hot side heat exchanger

According to the style of heat source and heat dissipation, the heat exchange can be classified into the following four categories.

As shown in Fig. 5, the four categories of thermal boundary conditions exist in thermoelectric applications. The most commonly investigated boundary condition (Fig. 5a) assume that both the hot and cold sides are isotropic at temperatures T_h and T_c, respectively. This condition is used in most studies, but has been rarely achieved in practical applications. However, the configurations (Fig. 5b, c and d) that replace one or both of the isotropic boundaries with convective media as sources or sinks for thermal power are more common in today's applications. Assuming the thermal power Q_h passes through the hot side of the module at temperature T_h and unconverted heat Q_c is dissipated at temperature T_c on the cold side. As described by Seebeck effect, this temperature difference $T_h - T_c$ induces a conductive thermal flux which consequently generates electricity. The amount of electrical power output R_{cx} is determined by temperature difference $T_h - T_c$ and the properties of thermoelectric materials.

The design of heat exchangers in this system uses Fig. 5c; it uses fluid-filled heat exchanger to absorb the heat from available heat sources and provides it to the TE modules for energy conversion. By

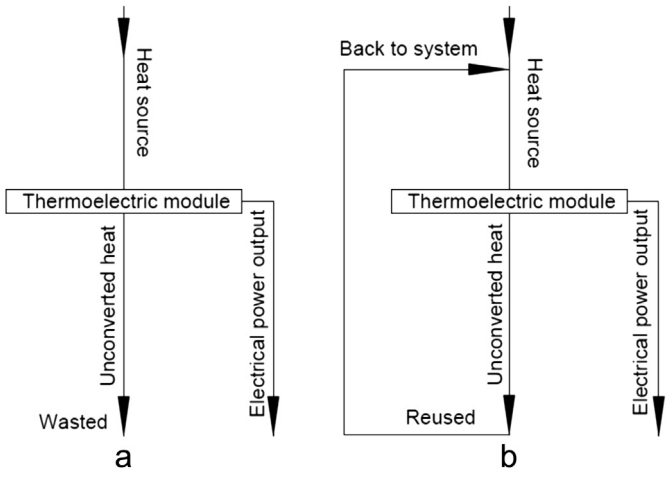

Fig. 4. Thermal cycle in the conventional thermoelectric power generation (a) and domestic TCS (b).

introducing the heat transfer oil, an even temperature distribution can be obtained on the hot side and the accommodation of dual or multiple heat source by bridging different thermal flux becomes possible.

The hot side heat exchanger absorbs the solar energy on the exterior surface which heats the heat transfer oil in the heat exchanger. Meanwhile, the boiler waste heat can be absorbed by the heat pipe heat exchanger which transfers the heat from the boiler flue gas to the oil. The whole system concept can be referred in Fig. 1.

In the experimental tests, the heat source is replaced by two round Ø6 mm × 100 mm electric heating elements with the maximum 100 W output which simulates the heat source at adjustable heat input. The cartridge heaters are inserted into the two aluminium tubes that are soldered to the side wall and enclosed in the tank, shown in Fig. 6. The maximum power output of electric cartridge heater is selected according to the maximum operating temperature of heat transfer oil and TE module. The electric heating elements heat the oil through the two aluminium tubes to avoid the direct contact with oil and electric elements which would cause the sealing issue. The amount of heat generated by the electric elements is then adjusted through a variable voltage transformer.

The use of heat transfer oil improves temperature distribution, eliminates hot spots on the TE module surface, and increases steady state performance and the reliability. However, it also increases thermal inertia of the system at the same time. Therefore, the optimum volume is determined by the amount of available heat. The impact to the system performance is discussed in subsection 4.2.4.

3.2. Cooling plate

In thermoelectric applications, the design of heat exchangers has found the important position in creating optimum thermal conditions for the great performance of thermoelectric applications. The cooling plate, which shoulders the responsibility of cooling the cold side surface of thermoelectric module, decides where and at what rate the heat output is dissipated into the environment or managed for other purposes. The former means the heat is dissipated in an unorganised way. It could either benefit the environment if the thermal environment needs it, or oppositely deteriorate the environment thermal condition by dissipating the unwanted heat to the surrounding. For example, in winter, this part of dissipated heat can only be used in a local area rather than used systematically for a larger space. In summer, this heat is unwanted for the environment. Heat dissipation to the environment only enlarges the cooling load for air conditioning. Good thermal management ensures the heat output, which represents a large proportion of the total absorbed heat because of the current low conversion efficiency, to be used in an organised way by managing the usage of heat output for other purposes. By effectively using these two parts of energy-power output and heat output, the heat utilisation efficiency could be tremendously enhanced.

Currently, the cooling methods generally include five types [26], which are liquid cooling, forced convection of air cooling, natural convection of air cooling, edge cooling and phase changing cooling. The cooling methods that have been used in thermoelectric power generations normally include natural convection of air [27], heat pipe, forced convection of air cooling (fan cooling) [17–19,28], and liquid cooling [21–24]. They can be categorised into active cooling (forced air/water cooling) and passive cooling (heat pipe and natural air convection). In previous researches, forced air cooling is the most used heat dissipation method. The fan cooling method is ineffective in achieving big temperature difference due to the low specific heat capacity of air [2]. Other disadvantages lie in extra

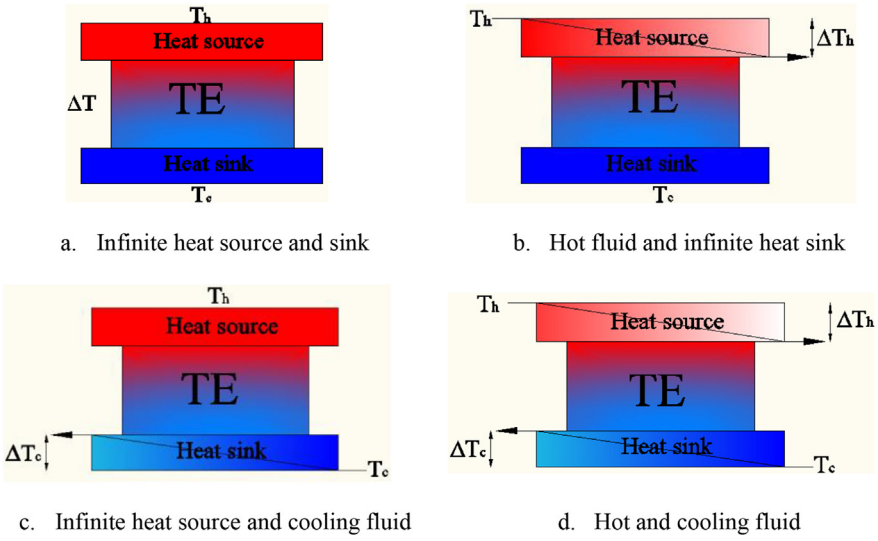

Fig. 5. Heat exchange types in thermoelectric applications.

electricity consumption, low reliability because of short fan life, noisy operation and low system efficiency caused by the unorganised heat dissipation.

In some applications, passive heat sinks like heat pipe or thermosyphonic are used at the cold side of thermoelectric generator [29,30]. The advantages of this method is energy saving and quiet due to its zero energy consumption and none moving parts compared to other methods that are related to the extra use of cooling fan. However, this cooling method, despite the advantages mentioned above, delivers low system efficiency by wasting the unconverted heat. Due to the low specific heat capacity of air, a heat sink with large area is needed for effective heat dissipation. It means relatively large space is needed in this type of application, unsuitable for the compact systems.

However, in the applications of cogeneration, however, rejected heat is recovered by circulating a fluid through a plate heat exchanger. The configuration of the plate heat exchanger is shown in Fig. 7. It is made of an aluminium block through which multiple branch channels are machined across the plate to emerge at both ends into a common header. The adoption of such a fluid flow looped structure enables the flow to "sweep" the whole heat transfer area with good temperature distribution on the surface, eliminating heat build-up and hot spots [31]. This design is characterised by a lower pressure drop compared with the current one of the most popular cooling plate design with embedded coiled tube (also called "cold plate"). The channel sizes are designed to comply with the required flow rate of feed water for nominal boiler operation.

Fig. 8 compares the experimental results of pressure drop of single channel (coiled tube cooling plate) and multi-channel cooling plates with 3 mm, 4 mm and 5 mm branch channel. Under the same flow rate, all the three MC cooling plates showed a lower pressure drop than the coiled tube cooling plate.

Fig. 9 shows the experimental result of cooling capacity and heat transfer coefficient of single channel cooling plate and multi-channel cooling plate with 3 mm branch channel. In the whole range of investigated flow velocity, an advantage in thermal performance of the multi-channel cooling plate over the single channel one is reported in this result (7.6%–9.4%).

In the numerical simulations to these two types of cooling plate design, an evener and lower temperature distribution on the interface with module surface, which is advantageous for the performance of thermoelectric generators, has been also obtained by employing this oriented cooling design. This can be explained by the "sweeping" effect of multiple branch channels which reduce the thermal accumulation shown in the "coiled" single channel cooling plate. The details of numerical results are not presented in this paper. However, this initial discovery further confirms the conclusion drawn in the experimental study that the multi-channel cooling plate introduced in this paper is more suitable for the domestic TCS as heat dissipation than the currently commercial coiled single channel cooling plate.

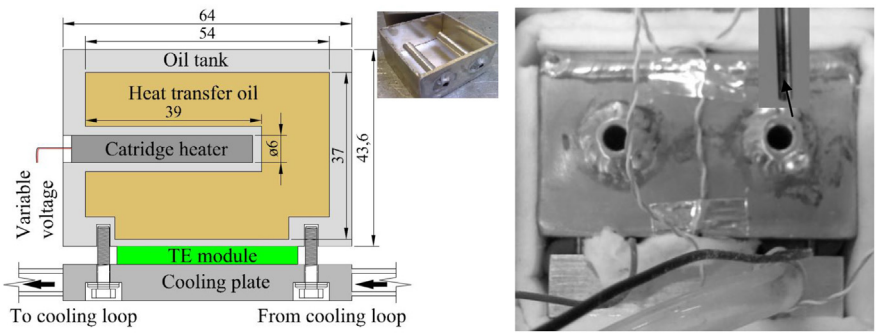

Fig. 6. Schematic diagram and photo of TCS with single module.

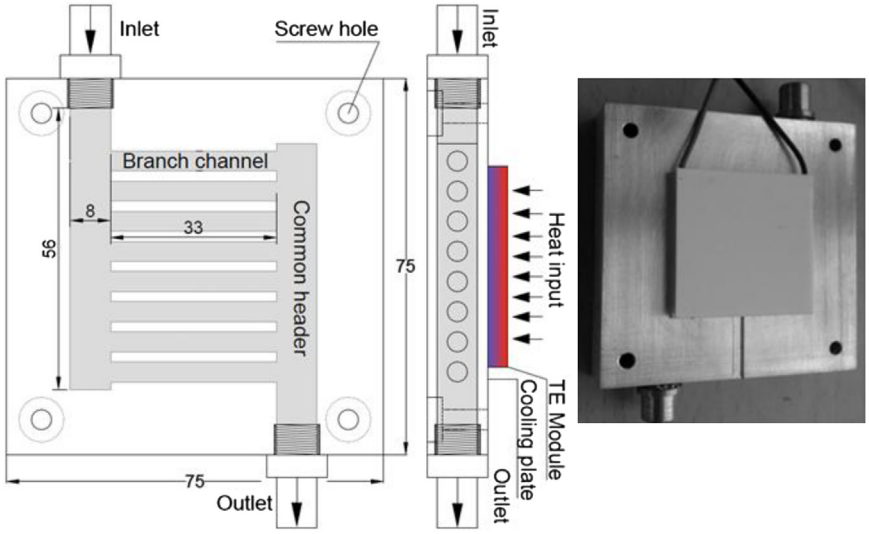

Fig. 7. Cooling plate for each thermoelectric module.

3.3. Mathematical analysis

The heat transfer in the co-generator assembly is simulated using lumped parameters. Heat flow from the heat source to the heat sink is shown in Fig. 10, where it shows that heat flow is mainly through a series of thermal resistances that define the heat source thermal resistance, R_{inth}, the TE thermal resistance, R_{te}, and the thermal resistance of the cooling plate and its interface with the TE, R_{cx} and R_{intc} respectively.

A parallel path for heat leakage through the insulation from the heat source to the heat sink is defined by the thermal conductance, $1/R_{ins}$, which is generally small and can be omitted.

The thermal performance of the co-generator is characterised by two main parameters namely the electrical conversion and overall thermal efficiency. The electrical conversion efficiency η is the ratio of the power output P to available heat input Q_i. The overall thermal efficiency η_{cog} is the ratio of the sum of power output P and recovered useful heat Q_o to the available heat input Q_i.

The power output, heat output and heat loss of the system can be expressed by Eq. (1), Eq. (2) and Eq. (3):

$$P = S^2\frac{(T_1 - T_2)^2}{R_{ex}} \tag{1}$$

$$Q_O = c\rho g(T_{outlet} - T_{inlet}) \tag{2}$$

$$\Delta T_{te} \tag{3}$$

In the test, electrical cartridge heaters are used to heat up the oil to the required temperature T_h. The tank size decides the time of heating the oil up to T_h. When the heat is supplied on the hot side, the total heat flux is split into two directions. One is flowing through thermoelectric module as Q_{sys} (some is for power generation and the rest is collected by heat sink), the other is lost into the ambient environment Q_{loss}, shown in Fig. 10. The equation showing the distribution of heat flux is,

$$Q_i = Q_{loss} + Q_{sys} \tag{4}$$

Assuming the temperature of inlet water of cooling plate is the same as the environment temperature, the thermal cycle of whole system can be explained by Fig. 10.

Generally, for a given system, the heat flux to the environment (heat loss) and through the system path should be proportional when the thermal resistance stays unchanged. However, Fig. 11 shows the thermal efficiency for 47 W heat input is higher than that given by 93 W.

Analysing the test data, it was found the module thermal resistance changed slightly with the operating temperature. As shown in Fig. 12, it shows a higher thermal conductivity was given by the smaller heat input. Consequently, Q_{sys} in Fig. 10 falls down due to the increased thermal resistance on the system side when it

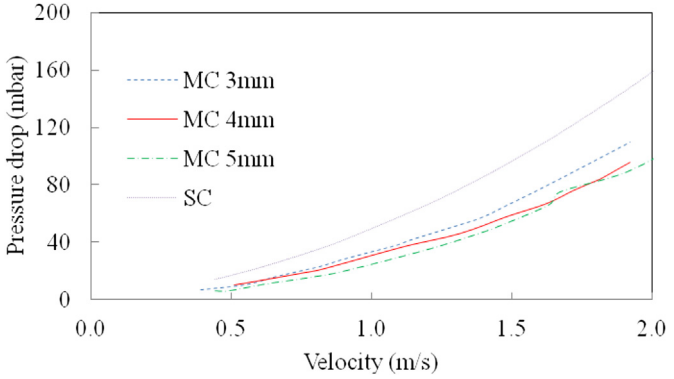

Fig. 8. Pressure drop comparison of single channel (SC) and multi-channel (MC) cooling plates.

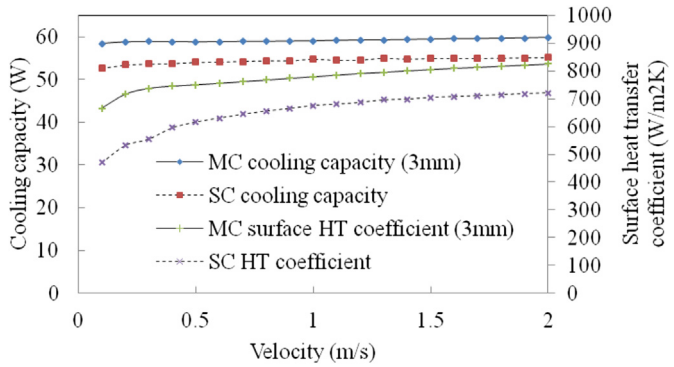

Fig. 9. Comparisons in cooling capacity and heat transfer coefficient of single channel (SC) and multi-channel (MC) cooling plates.

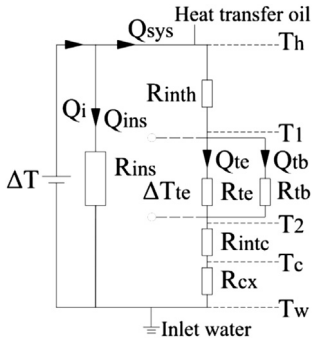

Fig. 10. Schematic diagram of heat flux distribution in single-stage TCS.

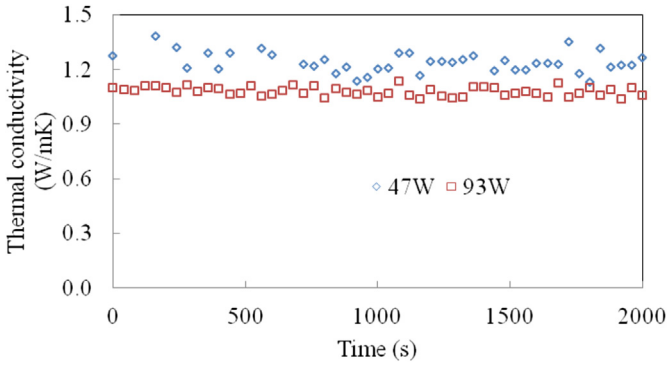

Fig. 12. Module thermal conductivity at the heat input of 47 W and 93 W.

operates at a higher heat input. Therefore, system thermal insulation should be designed according to the operating temperature level in reality.

4. Experimental tests

4.1. Description of a small scale test rig

A model-scale experimental prototype of a TE co-generator has been constructed and measurements of its performance have been carried out. The schematic diagram of the test rig is shown in Fig. 13. The TE block is composed of one thermoelectric module, a cold side and hot side heat exchanger. The module, made of semiconductor material Bi_2Te_3, has a dimension of 40 mm × 40 mm × 3.8 mm with 127 thermocouple elements. Thermal interface materials are placed at the interface of solid surfaces to enhance the heat transfer. Graphite and thermal grease are used at the hot side and cold side interface, respectively. Two cartridge heaters rated at 100 W are used to supply heat on the hot side. The heat supply to the TE module can be adjusted by changing the voltage input.

The TE module is cooled by circulating water through the multi-channel cooling plate and rejecting it through a fan cooled condenser. Compared to the single channel cooling plate, the multi-channel cooling plate creates lower temperature on the module cold side by achieving lower replacing rate. Therefore, the heating time length of water flow by the wall flow channel in the multi-channel cooling plate is longer, which leads the average temperature of TE cold side surface to be lower compared to the single channel cooling plate. The temperature at the heat source and heat sink is measured by K-type thermocouples and the flow rate of cooling water is measured by a flowmeter. The thermocouples were located in slots machined on the surface of the heat exchangers. The temperature, flow rate and voltage are recorded by a DT500 series 3 datataker. A decade resistance box ranging from (1 Ω–100 kΩ) is connected to TE module to provide adjustable external load.

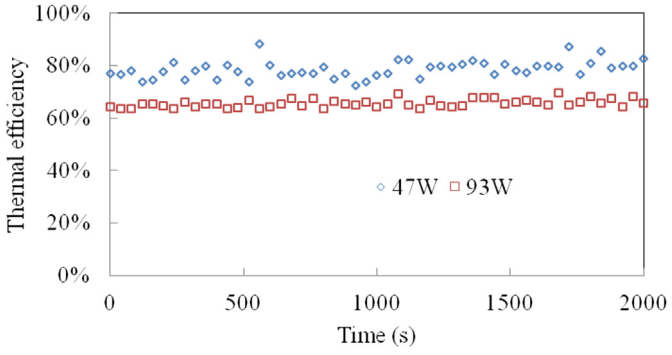

Fig. 11. Thermal efficiency at the heat input of 47 W and 93 W.

4.2. Performance analysis

4.2.1. Electric performance

At steady state when a temperature difference is established across the TE module, the theoretical maximum power output from the module is given by Eq. (5):

$$P = \frac{V_o^2}{4R_L\left(\frac{V_o}{V} - 1\right)} \tag{5}$$

In this work, a commercial TE module was tested with the heat input at 47 W and 93 W. The optimum external load electrical resistance was first determined which corresponds to the maximum power output. This is achieved when the internal electrical resistance of the TE module equals to that of the external resistance.

Fig. 14 shows the open voltage and maximum power output of the system when it operates at different temperature difference. Open voltage shows a linear correlation with the temperature difference across the thermoelectric module, while a nonlinear correlation is shown between the maximum power output and temperature difference. Both of them rise alongside the increase of operating temperature difference.

The system voltage output has been tested when the external resistance is loaded at 1 Ω, 2 Ω, 3 Ω, 4 Ω, 5 Ω, 6 Ω, 7 Ω, 8 Ω, 9 Ω, 10 Ω,

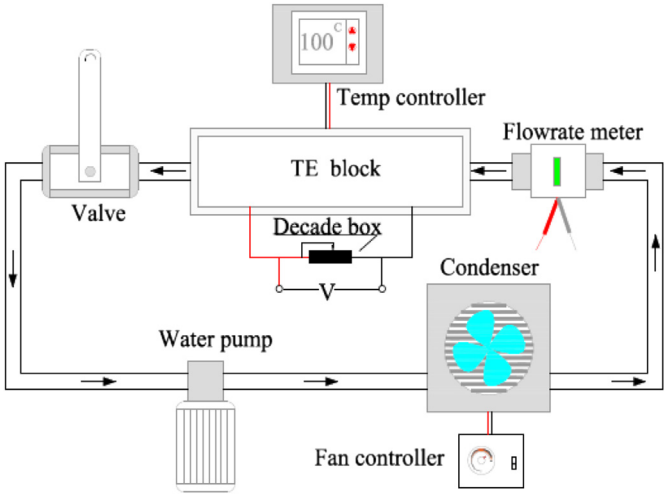

Fig. 13. Schematic diagram of small scale co-generator test rig.

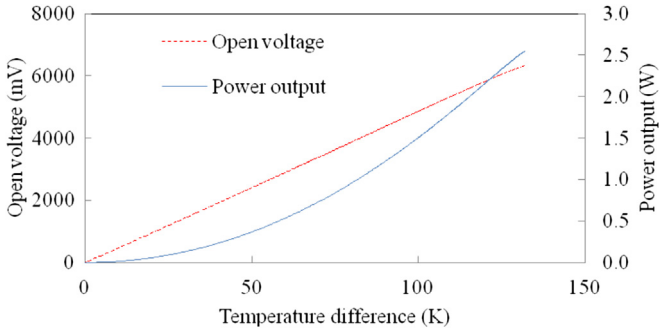

Fig. 14. System open voltage output and power output vs. temperature difference.

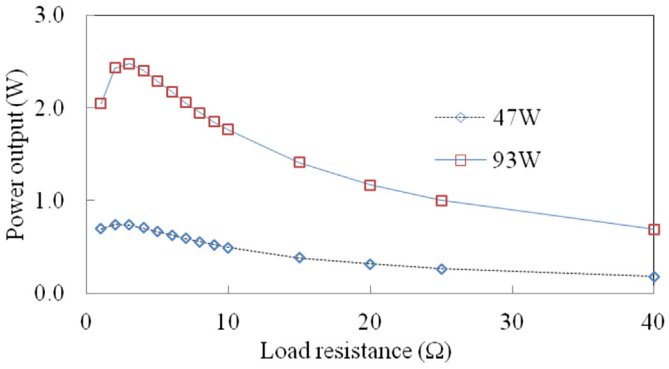

Fig. 16. Power output at different load resistance.

15 Ω, 20 Ω, 25 Ω, 30 Ω, 35 Ω and 40 Ω, respectively. This adjustment has been achieved by using decade box. Fig. 15 shows the voltage output of the system loaded with different resistance value. This has been tested with the integration of the cooling plate with 3 mm, 4 mm and 5 mm branch channel, but only the result of the 3 mm one is presented to demonstrate the general trend. The curve reports the voltage output rises along with increased external electrical resistance load. However, the highest value of voltage output does not correspond to the maximum power output.

Fig. 16 shows the measured power output of the TE module as a function of the external load resistance. It can be seen that maximum power output is achieved for an electrical resistance of 2 Ω and 3 Ω when the heat is supplied at 47 W and 93 W. The corresponding temperature of heat source and heat sink for the 47 W and 93 W is 102 °C/31 °C and 166 °C/34 °C, respectively. The maximum power output corresponds to a terminal voltage of 1.2 V and load current 0.61 A for the 47 W and 2.73 V and 0.91 A for the 93 W.

The electrical efficiency of the TE module can be determined from Eq. (6):

$$\eta = \frac{\Delta T}{T_1}\left(\frac{\sqrt{Z\overline{T}+1}-1}{\sqrt{Z\overline{T}+1}+1-\Delta T/T_1}\right) \tag{6}$$

The TE module electrical performance was determined under different temperature gradients by varying the heat source temperature while the heat sink temperature was kept constant. Fig. 17 shows the maximum power output and conversion efficiency against the heat source temperature. The spots fluctuating around the main trend line can be omitted due to experimental errors. The result shows the conversion efficiency is determined by the temperature difference. The bigger the temperature difference is, the higher the conversion efficiency. In this study, the highest temperature difference was achieved at 130 °C, which gives about 3.9% conversion efficiency, higher than the 2% with 200 °C temperature difference mentioned in Ref. [18] based on the same thermoelectric material, Bi_2Te_3.

As previously mentioned, the best system performance needs to produce the maximum net energy gain, which means the need of delivering a maximum cooling capacity in the price of the lowest pressure drop. Therefore, the electric performance, thermal performance and hydraulic performance are investigated at different flow rate to understand the system performance under different flow conditions. For each velocity change, the test was run until its output stabilised, which took between 1 and 2 min counting from the beginning. In order to obtain the reasonably accurate result, the time length for each velocity range is set at 10 min. The results are introduced in subsection 4.2.1, 4.2.2 and 4.2.3, respectively.

As shown in Fig. 18, when the inlet flow velocity of the cooling plate decreases in the range of 0.12 m/s-0.59 m/s, the TE cold side temperature ("CS" in the figure) increases. This can be explained by the longer heating time when the flow velocity is low, which makes the average coolant temperature in the cooling plate is higher. This consequently makes a higher temperature at the TE cold side. However, this hardly affects the temperature difference across the module which leads to a stable output of electrical power in the system. The reason why the temperature difference stays nearly unchanged can be explained by the constant heat flow through the module when the heat input from the electric heater is unchanged. The hot side temperature rises gently when the cold side temperature increases, the impact to the heat loss through the insulation is not significant enough to affect the temperature difference across

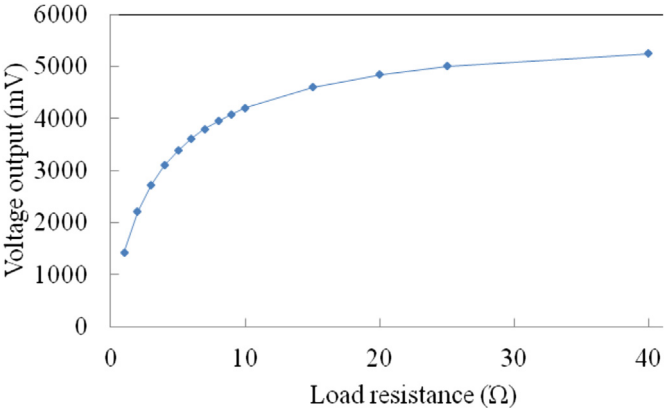

Fig. 15. Voltage output at different load resistance of the system integrated with the cooling plate with 3 mm branch channel.

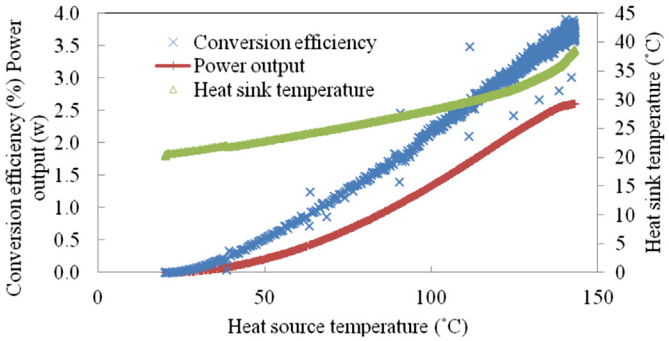

Fig. 17. Maximum power output and conversion efficiency vs. Heat source temperature.

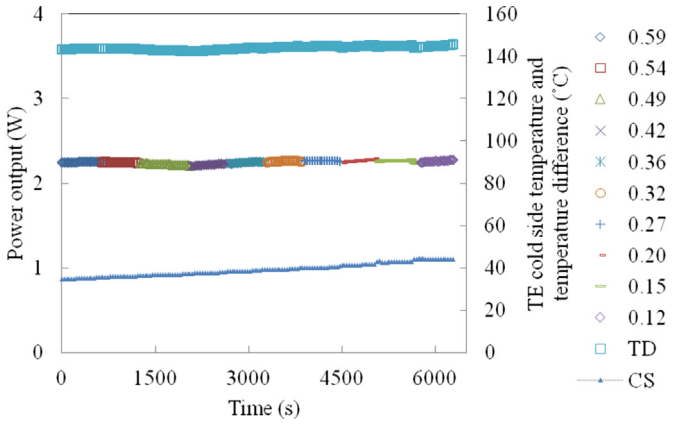

Fig. 18. Power output, TE cold side temperature (CS) and temperature difference (TD) under different inlet coolant velocity.

the module. It does not impose a big change to the temperature difference. This might mislead the reader to the conclusion that the inlet coolant temperature does not affect the system power output. In the specific test that looks into the impact of inlet coolant temperature to the system performance, it was found that the system heat output and power output was enhanced by 35% and 13% when the inlet coolant temperature is decreased from 37 °C to 27 °C with other boundary conditions staying unchanged.

4.2.2. Thermal performance

At steady state the thermal performance of the TE co-generator was determined by measuring heat recovered for different heat source temperatures when the heat sink temperature remains constant.

The thermal efficiency, which is defined by the ratio of the sum of power output and heat output to the total heat input from the electric heater, is reported in Fig. 11, which shows the thermal efficiency is up to 80% which is not experimentally presented in other studies.

An average value of heat output was calculated from the test results in each time length, the result is shown in Fig. 19. The accuracy of the results shown below has been further proved by another set of experiment which delivers the same system performance. The temperature rise of the coolant through the cooling plate increases along with the decrease of inlet flow velocity. The heat output goes up slightly along with the increase of the inlet flow velocity, as shown in Fig. 19.

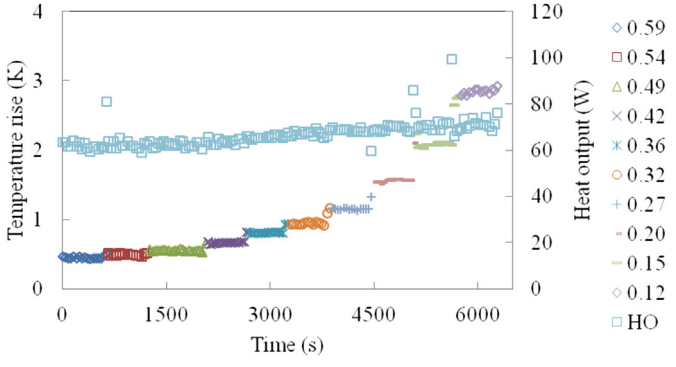

Fig. 19. Temperature rise of coolant that flows through the cooling plate at different inlet coolant velocity.

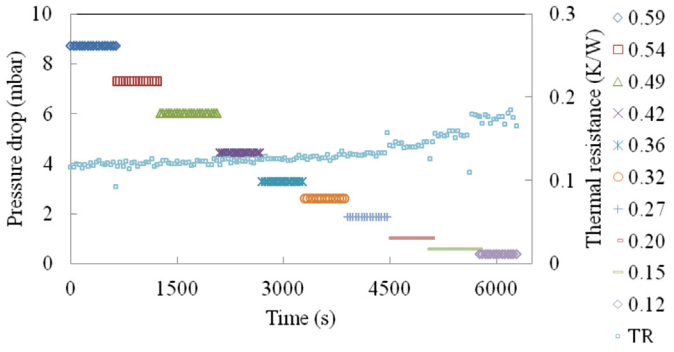

Fig. 20. Pressure drop and thermal resistance of cooling plate under different inlet coolant velocity.

4.2.3. Hydraulic performance

Considering the impact of the coolant velocity at the cooling plate inlet to the power and heat output discussed subsection 4.2.1 and 4.2.2, we can conclude that a lower coolant velocity at the cooling plate inlet can achieve a bigger value of overall energy output. The pressure drop caused by the cooling plate represents the energy input when the cooling plate meets the cooling target of the TE module. The pressure drop at different inlet coolant velocity is shown in Fig. 20. It shows that the pressure loss drops significantly when the inlet coolant velocity decreases. Namely, a smaller energy input is required at a lower coolant velocity, which consequently increases the system's net energy gain.

Based on the aforementioned results and discussions, it can be concluded a lower flow rate in the range of 0.12 m/s–0.59 m/s obtains a better system performance. However, the flow rate needs to be designed in combinations with nominal flow rate required by the host device and the integration of cooling plate.

4.2.4. Dynamic thermal response of the system

The use of a thermal fluid (heat transfer oil) to recover heat from multiple waste heat sources and channelling it to the thermoelectric hot plate introduces further design challenges in minimising the thermal inertia of the system. The time required to heat the oil in the TE module hot plate heat exchanger to the designed temperature can be determined by Eq. (7):

$$t = \frac{C_o \rho_o V (T_h - T_a)}{Q_i} \tag{7}$$

The oil temperature was measured for a heat exchanger storage capacity of 144 ml and at the design condition of a 100 W heat input, the dynamic response of the system is shown in Fig. 21.

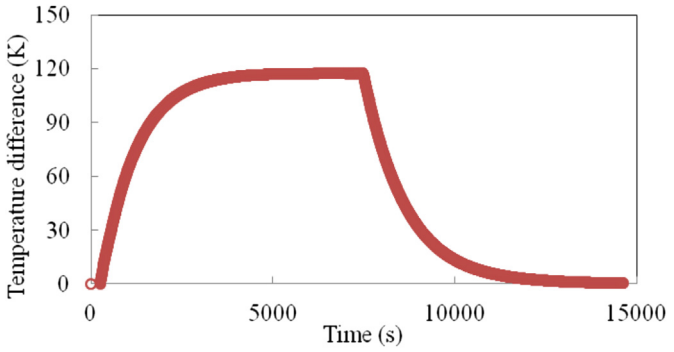

Fig. 21. Dynamic thermal response of the system.

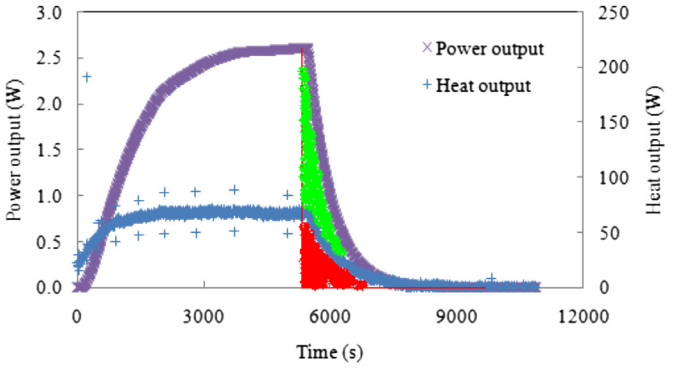

Fig. 22. Power output and heat output in a test cycle.

Fig. 21 shows that when the oil is heated from ambient temperature it takes about 3000 s to reach steady state temperature of 120 °C. This represents a time constant of the system to reach the steady state; it is desirable to have a fast response system. However, in applications for exploitation of renewable energy sources, energy storages capability could present a potential advantage. The thermal response of the system after the removal of the heat source is shown in Fig. 22. It can be seen that during the cooling down of the stored oil, heat could still be recovered from the system, though the power output would be limited by the voltage output level. Removing the effect of voltage level, the total power output generated during the cooling phase amounts to 1.7 Wh and is given by the sum of shaded area of green and red. The total heat output produced during the cooling phase amounts to 10.2 Wh and is given by the shaded area of red colour.

4.3. Discussion

The common heating facilities in residential houses normally include domestic boiler, stoves and fireplaces, most of which produces a considerable amount of waste heat at a high grade temperature, presenting thermoelectric applications with great opportunity to improve overall energy efficiency of the domestic building. This study chooses to investigate small scale TCS to demonstrate the practicality and capability of enhancing domestic energy utilisation efficiency by using the thermoelectric cogeneration concept. Based on a simulated steady state heat source, it is intended to show the potential of changing the dilemma of low energy efficiency in conventional thermoelectric generations, which was proved by the experimental results. In order to tackle the issues existing in real applications, the design needs to focus on integrating thermoelectric system with the existing facilities from the following aspects:

1. An effective design of hot side heat exchanger should capture the waste heat efficiently but without consuming much energy or significantly influencing the performance of host facilities.
2. The design needs to comply with the nominal conditions which were originally tuned by the boiler manufacturer.
3. The availability of heat sources varies with the season, weather and domestic heating demand. The system performance under dynamic heat input is an advanced topic that needs to be further investigated and this study conducted under steady heat input paves the fundamental path for it.

5. Conclusion

This study, based on experimental investigations conducted on a model scale prototype, has pointed a possible direction of using thermoelectric technology with much higher energy utilisation efficiency in residential house-domestic TCS. The system performance has been analysed from four aspects, electric performance, thermal performance, hydraulic performance and dynamic thermal response of the system. It was found that the matched externally loaded electrical resistance that gives maximum power output varies with the operating temperature. The estimated explanation goes to the temperature-dependent internal electrical resistance, which also explains the reason why thermal efficiency is varied slightly by the operating temperature. This needs to be considered in the design of maximum power point tracking system for thermoelectric generations. The use of fluid-filled hot side heat exchanger endows the system the capability of storing and spreading heat. However, the volume of the fluid, which is heat transfer oil in this study, needs to be carefully designed according to the available amount of heat to reduce/eliminate thermal inertia caused by the fluid. Originally designed to be used in residential house installed with domestic boiler, this system concept is also applicable to other sectors or areas where the combustion appliances are used and preheating is needed.

Nomenclature

A	exterior surface area of heat source m^2
C	specific heat capacity of water j/kg K
C_o	specific heat capacity of heat transfer oil (2500) j/kg K
g	gravitational constant m/s^2
G	water flow rate m^3/s
h	heat transfer coefficient W/m^2K
P	maximum power output W
Q_{bw}	available boiler waste heat W
Q_i	heat input W
Q_{loss}	system heat loss to the ambient environment W
Q_o	heat output W
Q_{solar}	available solar power W
Q_{sys}	effective heat to the system
r_{ex}	external electrical resistance Ω
r_L	electrical resistance of external load Ω
R_{inth}	thermal resistance of hot side heat exchanger m^2K/W
R_{intc}	thermal resistance of cooling plate m^2K/W
R_{ins}	thermal resistance of insulation m^2K/W
R_{te}	module thermal resistance m^2K/W
S	Seebeck coefficient V/K
t	Heated time s
T_a	ambient temperature °C
T_c	heat sink temperature °C
T_h	heat source temperature °C
$\overline{T}$	average operating temperature °C
T_1	module hot side temperature °C
T_2	module cold side temperature °C
V_o	open circuit voltage output V
V	loaded voltage output V
T_{outlet}	outlet water temperature °C
T_{inlet}	inlet water temperature °C
ZT	dimensionless figure of merit
Z	figure of merit K-1

Greek symbols

η	conversion efficiency
η_{cog}	Overall thermal efficiency
λ	thermal conductivity W/m K
ρ	water density kg/m3
ρ_o	density of heat transfer oil (0.888) g/ml
σ	electrical conductivity S/m
ΔT	temperature difference across thermoelectric module °C

References

[1] Boiler efficiency database. http://www.sedbuk.com/, 2009.
[2] C.T. Hsu, G.Y. Huang, H.S. Chu, B. Yu, D.J. Yao, Experiments and simulations on low-temperature waste heat harvesting system by thermoelectric power generators, Appl. Energy 88 (2011) 1291–1297.
[3] N.D. Love, J.P. Szybist, C.S. Sluder, Effect of heat exchanger material and fouling on thermoelectric exhaust heat recovery, Appl. Energy 90 (2012) 322–328.
[4] T. Kajikawa, I.M. Ito, I. Katsube, E. Shibuya, Development of thermoelectric power generation utilising heat of combustible solid waste, in: Proc. 13th Int. Conf. on Thermoelectrics, Kansas City, USA, 1994, pp. p.314–318.
[5] T. Kajikawa, Thermoelectric power generation systems recovering heat from combustible solid waste in Japan, in: Proc. 15th Int. Conf. on Thermoelectrics, Pasadena, USA, 1996, pp. 343–351.
[6] X.L. Gou, H. Xiao, S.W. Yang, Modelling, experimental study and optimization on low-temperature waste heat thermoelectric generator system, Appl. Energy 87 (2010) 3131–3136.
[7] N.F. Gueler, R. Ahiska, Design and testing of a microprocessor-controlled portable thermoelectric medical cooling kit, Appl. Therm. Eng. 22 (2002) 1271–1276.
[8] S. Chatterjee, K.G. Pandey, Thermoelectric cold-chain chests for storing/transporting vaccines in remote regions, Appl. Energy 76 (2003) 415–433.
[9] D.M. Rowe, Applications of nuclear-powered thermoelectric generators in space, Appl. Energy 40 (1991) 241–271.
[10] A.I. Boukai, Y. Bunimovich, J. Tahir-Kheli, J.K. Yu, W.A. Goddard, J.R. Heath, Silicon nanowires as efficiency thermoelectric materials, Nature 451 (2008) 168–171.
[11] A.I. Hochbaum, R.K. Chen, R.D. Delgado, W.J. Liang, E.C. Garnett, M. Najarian, A. Majumdar, P.D. Yang, Enhanced thermoelectric performance of rough silicon nanowires, Nature 451 (2008) 163–167.
[12] J.P. Heremans, V. Jovovic, E.S. Toberer, A. Saramat, K. Kurosaki, A. Charoenphakdee, S. Yamanaka, G.J. Snyder, Enhancement of thermoelectric efficiency in PbTe by distortion of the electronic density of states, Science 321 (2008) 554–557.
[13] K.F. Hsu, S. Loo, F. Guo, W. Chen, J.S. Dyck, C. Uher, T. Hogan, E.K. Polychroniadis, M.G. Kanatzidis, Cubic AgPbmSbTe2+m: bulk thermoelectric materials with high figure of merit, Science 303 (2004) 818–821.
[14] D.M. Rowe, Review thermoelectric waste heat recovery as a renewable energy source, Int. J. Innovat. Energy Syst. Power 1 (1) (November 2006).
[15] Zeng G, Bahk JH, Bowers JE, Lu H, Zide JMO, Gossard AC, Singh R, Bian ZX, Shakouri A, Singer SL, Kim W, Majumdar. Power generator modules of segmented Bi2Te3 and ErAs: (InGaAs)1-x(InAlAs)x. J. Electron. Mater. http://dx.doi.org/10.1007/s 1664-008-0435-2.
[16] Caillat T, Fleurial JP, Borshchevsky A. Development of High Efficiency Thermoelectric Generators Using Advanced Thermoelectric Materials, Albuquerque, New Mexico, USA, 1998.
[17] A. Killander, J. Bass, A stove-top generator for cold areas, in: 15th Int. Conf. on Thermoelectrics, Pasadena, USA, 1996, pp. 390–393.
[18] D. Champier, J.P. Bedecarrats, M. Rivaletto, F. Strub, Thermoelectric power generation from biomass cook stoves, Energy 35 (2010) 935–942.
[19] R.Y. Nuwayhid, D.M. Rowe, G. Min, Low cost stove-top thermoelectric generator for regions with unreliable electricity supply, Renewable Energy 28 (2003) 205–222.
[20] D. Mastbergen, B. Willson, S. Joshi, Producing Light from Stoves Using a Thermoelectric Generator, in: Report of the Energy Conversion Lab Colorado State University, 2005. Available at: www.vrac.iastate.edu/ethos/files/ethos2005/pdf/mastbergen.pdf.
[21] D. Allen, J. Wonsowski, Thermoelectric self-powered hydronic heating demonstration, in: Proc 16th Int Conf on Thermoelectric, Dresden, Germany, 1997, pp. 571–574.
[22] D. Allen, W. Mallon, Further development of “self-powered boilers”, in: Proc 18th Int Conf on Thermoelectrics, Baltimore, USA, 1999, pp. p.80–83.
[23] G. Min, D.M. Rowe, Symbiotic application of thermoelectric conversion for fluid preheating/power generation, Energy Convers. Manage. 43 (2002) 221–228.
[24] X.F. Zheng, Y.Y. Yan, K. Simpson, A potential candidate for the sustainable and reliable domestic energy generation – thermoelectric cogeneration system, Appl. Therm. Eng. 53 (2013) 305–311.
[25] K. Qiu, A.C.S. Hayden, A natural-gas-fired thermoelectric power generation system, J. Electron. Mater. 38 (2012) 1315–1319.
[26] D.S. Steinberg, Cooling Techniques for Electronic Equipment, John Wiley & Sons, United States of America, 1991.
[27] R.Y. Nuwayhid, A. Shihadeh, N. Ghaddar, Development and testing of a domestic woodstove thermoelectric generator with natural convection cooling, Energy Convers. Manage. 46 (2005) 1631–1643.
[28] Dan Mastbergen, Bryan Willson, Sachin Joshi, Producing Light from Stoves using a Thermoelectric Generator, 2005.
[29] R.Y. Nuwayhid, R. Hamade, Design and testing of a locally made loop-type thermosyphonic heat sink for stove-up thermoelectric generators, Renewable Energy 30 (2005) 1101–1116.
[30] X. Yang, Y.Y. Yan, D. Mullen, Recent developments of lightweight, high performance heat pipes, Appl. Therm. Eng. 33–34 (2012) 128–134.
[31] X.F. Zheng, et al., J. Phys. Conf. Ser 395 (2012) 012062.